Вестник Физико-технического института
Крымского федерального университета имени В. И. Вернадского
Том 1 (67–69). № 2. 2017. С. 19–44
Journal of Physics and Technology Institute of V. I. Vernadsky Crimean Federal University
Volume 1 (67–69). No. 2. 2017. P. 19–44

УДК 535.015

FRACTIONAL OPTICAL VORTICES: STABILITY DECAY AND TRANSFORMATION

Volyar A. V., Alexeyev C. N., Egorov Yu. A., Akimova. Ya. E.**

V. I. Vernadsky Crimean Federal University, Vernadsky Prospekt 4, Simferopol 295007, Russia
****E-mail: yana_akimova_1994@mail.ru***

In this paper we studied the shaping and evolution of singular beams bearing optical vortices with fractional topological charges both in uniform and non-uniform anisotropic media. Starting from representation of the fractional-order vortex states as a superposition of an infinite number of integer-order vortices with certain energy distributions (the vortex spectra) we showed that the smooth wave front of the fractional vortex beam can either decay into an asymmetric array of integer-order vortices or, vice versa, the array of optical vortices can form a smooth helicoid-shaped wave front. We showed that by superimposing a finite number of the fractional-order vortex beams one can shape symmetric singular beams with arbitrary valued topological charges. We demonstrated that in biaxial crystals under the condition of the conical diffraction the fractional-order vortices are unstable. We also demonstrated that the circular fiber array with a space-variant birefringence is an appropriate medium for fractional-order vortex beams.
Keywords: optical vortices, fractional topological charges, the fractional-order supermodes, hidden phase, the array of optical vortices.

PACS: 41.85. –p

INTRODUCTION

The unexpected prediction of vortices with half of a quantum unit of circulation in superfluid ^3He in the 1970s [1] at first provoked bewilderment among physicists because the problem was far from an obvious understanding. The fact is that the quantized circulation is connected with a superfluid flow and can have integer values only. For a long time, that prediction had been considered as a mathematical misunderstanding until J. Jang et. al. [2–4] have experimentally revealed half-quantum vortices in different condensed-matter systems from Bose-Einstein condensates to spin-triplet superconductors. To match the experimental results of the half-integer circulations with a generally accepted conception, the deficient phase π (a half-integer order of the circulation) came to be called the “hidden phase” that is not connected with the circulation of the mass current but is induced by the circulation of the spin current in Cooper pairs [4]. In other words, the spin-orbit interaction plays here the key part.

At last, there appeared a new approach for describing such physical processes based on analogy between spinor Bose-Einstein condensates and singular optical systems (see e.g. [5] and references therein).

At the same time, the optical states with fractional orders of the energy circulation are not so a drastic problem for flows of optical fields both in scalar and vector cases as it turns out to be for the superfluid cases (Fermi liquids). Nevertheless, propagation processes of singular beams bearing optical vortices with fractional-order topological charges face also the key questions of a structural stability of optical states under propagation or other negligibly small perturbations.

Past recent years of singular optic's [6] development have been marked by the surge of interest to optical vortices with fractional topological charges [7, 18]. The first announcement of the fractional-order vortex instability in principle was reported by Soskin et al [7, 8] for the vortices produced by a computer-generated hologram while the vortices propagate in free space. The authors observed experimentally evolution of vortex beams with different half-integer order topological charges. If the vortex beam at the hologram has a nearly C-shaped form, far from the hologram the beam breaks out onto a great number of integer-order vortices.

Later, Berry starting from analogy with the Aharonov-Bohm effect in quantum mechanics and hydrodynamics [9] has theoretically shown the splitting of an optical vortex of the fractional-order into infinite chain of the integer-order vortices [10]. He caught sight of a deep analogy between the quantum and the optical singularities. Besides, Berry denoted that the fractional-order vortex propagation results inevitably in decaying the initial phase structure in free space, i.e. the fractional-order vortex beams are structurally unstable ones under the propagation.

These reports stimulated a new chain of theoretical and experimental investigations [11−15] that confirmed the decay of fractional-order vortices into an infinite number of integer-order vortices. Although most of mathematical models of the fractional vortices is based on the Bessel-Gaussian beam presentation (see e.g. [13, 14], authors of the paper [15] supplemented the analysis with the Laguerre-Gaussian beams. Difference between these approaches lies in different contribution of the individual integer-order vortices in the complex field when the fractional-order beam evolves through the optical medium. Some typical features of such dynamical transformations were considered experimentally in the recent paper [18].

On the other hand, authors of the paper [17] found out a strange behavior of the vortex-beam with a half-order topological charge for the erf-Gaussian ($erf-G$) beams. The smooth wave front of the fractional vortex beam can either decay into an asymmetric array of integer-order vortices or, vice versa, the array of optical vortices can be gathered together forming a smooth wave front with a helicoid-shaped phase distribution.

Authors of the paper [21] remarked also unusual behavior of the orbital angular momentum l_z (OAM). At first glance it seems that the fractional-order vortex topological charge is an indicator of the OAM of singular beams at least records nearest values to its physical quantity. In some first papers [14, 27] authors obtained a nearly linear dependence between l_z and a topological charge p on the base of assessed theoretical results. However, the computer simulation of the process and physical analysis [21] revealed a complex behavior of the function $l_z(p)$. Small values of the charge $p<10$ correspond to a nearly linear dependence $l_z \quad p$ with a small amplitude of oscillations. The growth of the value $p>10$ results in increasing the amplitude of oscillations between the values $l_z = \mathrm{int}\,eger(p)$ and $p=0$. The presented results are evidence of a complex interference coupling between a great numbers of the integer-order vortices in a fractional-order vortex beam.

One more unexpected property of the fractional-order vortex beams revealed the authors of the paper [16]. They tried to answer experimentally the question: can the fractional-order vortex-beams control the states of the integer-order ones? They achieved a success using two beams: the pump and probe ones.

The pump beam is of a topological dipole field consisting of two ½-order vortices with opposite signs of their charges. The pump beam lays a course in a nonlinear medium for the probe singular beam of a smaller intensity. Changing parameters of the dipole they can steer the state of the probe beam. In fact, the fractional-order topological dipole is not destroyed inside the nonlinear medium forming the waveguide channel for the probe beam.

1. FREE SPACE PROPAGATION OPTICAL QUARKS

As a rule, a beam field in a complex optical system contains a lot of simple composition Laguerre-Gaussian (LG), Hermit-Gaussian (HG), Bessel-Gaussian (BG) etc beams bearing an energy-limited optical flux. Each element of these mathematical constructions is an optical vortex-beam bearing an integer-order topological charge. Some of such beam combinations possess of extraordinary properties. The singular beam behavior depends on the energy distribution among the integer-order vortices and their phase parameters i.e. a spectral density $\rho(p)$ of optical vortices. A striking example is a fractional-order vortex beam. Its properties are defined by both the value of the topological charge p and type of its complex amplitude (BG, LG, etc).

In the following sub-sections, we set a task to uncover the basic properties of different types of the fractional-order vortex beams and to build up from them the integer-order vortex beams.

A. Optical quarks as a fractional optical vortex

Let us consider, at first, typical vector supermodes in free space or a uniform isotropic medium made up of the Bessel-Gaussian beams. We focus our attention on monochromatic wave beams with the carrier frequency ω that enables us to exploit the vector Helmholtz equation for the vector potential $\mathbf{A}$ under the condition of Lorentz gauge [17]. The electric $\mathbf{E}$ and magnetic $\mathbf{H}$ fields can be defined as

$$\mathbf{E} = ik\left[\mathbf{A} + \frac{1}{k^2}\nabla\left(\nabla\cdot\mathbf{A}\right)\right],\ \mathbf{H} = \nabla\times\mathbf{A}, \tag{1}$$

with the wavenumber k.

Our interest is the paraxial approximation where $\left|\partial_z^2\mathbf{A}\right| << \left|k^2\mathbf{A}\right|$ so that the longitudinal components E_z and H_z can be expressed in terms of the transverse $\mathbf{E}_\perp$ and $\mathbf{H}_\perp$ ones

$$E_z \approx \frac{i}{k}\nabla_\perp \cdot \mathbf{E}_\perp, \;\; H_z \approx \frac{i}{k}\nabla_\perp \cdot \mathbf{H}_\perp, \; \nabla_\perp \equiv \mathbf{e}_x\partial_x + \mathbf{e}_y\partial_y. \tag{2}$$

For the beam propagating along the $z-$axis of the complex amplitude $\mathbf{A}$ of the vector potential $\mathbf{A} = \mathbf{A}(x, y, z)e^{ikz}$ obeys the paraxial wave equation

$$\left(\nabla_\perp^2 + 2ik\partial_z\right)\mathbf{A}_\perp = 0 . \tag{3}$$

The choice of the vector $\mathbf{A}$ is defined by a type of the wave beam. If we take, for example, the vector $\mathbf{A}$ to be directed along the $x-$axis (a linearly polarized basis) $\mathbf{A} = \mathbf{e}_x A_\perp \exp(ikz)$ then the solution to the vector wave equation is reduced to the scalar equation (3) for the function $\Psi(x, y, z) = A_\perp$ with the solution [20]

$$\Psi = NF(X,Y)G(x, y, z), \tag{4}$$

where

$$G(x, y, z) = \exp\left(i\frac{k r^2}{2Z}\right)/Z \tag{5}$$

stands for the Gaussian envelope, $Z = z - iz_0$, $z_0 = kw_0^2/2$ is the Rayleigh length with the radius of the beam waist w_0, $X = x/Z, Y = y/Z$, $N = w_0 \exp\left(-\frac{K^2}{2ikZ}\right)$, $r^2 = x^2 + y^2$ and K is the arbitrary beam parameter that can take on both the real and complex values.

At the same time the function $F(X,Y)$ obeys the two dimensional Helmholtz equation

$$\left(\frac{\partial^2}{\partial X^2} + \frac{\partial^2}{\partial Y^2} + K^2\right)F = 0. \tag{6}$$

In the cylindrical coordinates the solution to the equation (6) can be written as

$$F_p(R,\varphi) = \int_0^{2\pi} \exp\left\{i\left[p\varphi' - KR\cos(\varphi' - \varphi)\right]\right\}d\varphi', \tag{7}$$

Here the parameter $p \in (-\infty, \infty)$ is arbitrary real value, $R^2 = X^2 + Y^2$. The real part of the parameter K is connected with the half angle θ of the plane wave's cone of the Bessel beam.

Such a representation of the beam charge $p \in (-\infty, \infty)$ enables us to expand any regular complex beam into the series over different fractional-charged optical vortices just as it can be presented in the form of the series over different integer-order charged optical ones.

To obtain the explicit form of the function F_p in (7) let us use the Fourier transformation

$$e^{ip\phi} = \frac{e^{i\pi p}\sin(\pi p)}{\pi} \sum_{m=-\infty}^{\infty} \frac{e^{im\phi}}{p-m}. \tag{8}$$

The parameter p here can be regarded as a fractional topological charge, that is responsible for the array of the integer-order vortices with topological charges $m = -\infty ... -1, 0, 1, .. + \infty$ with the spectral vortex density $\rho(p) = (p-m)^{-1}$. When $p = m$ all terms of the series vanish except the term $e^{im\phi}$. In a general case the function $\rho(p)$ can be defined by a preassigned way as, for example, in the paper [15] for Laguerre-Gaussian beams, but for our purposes we restrict its dependence to the simplest case of $\rho(p) = (p-m)^{-1}$.

On the other hand the definition of the Bessel function is

$$2\pi i^m J_m(KR) = \int_0^{2\pi} \exp\{i[m\phi + K\cos\phi]\} d\phi \tag{9}$$

with $\phi = \varphi' - \varphi$. As a result, we find

$$|p\rangle = \Psi(r, \varphi, z, p) = 2NG(r, z)\sin(\pi p)\, e^{i\pi p} \sum_{m=-\infty}^{\infty} \frac{i^m e^{im\varphi}}{p-m} J_m(KR), \tag{10}$$

Thus, the fractional topological charge p can serve as a global parameter of the complex optical beam. The obtained equation implies two possible propagation processes depending on the value of the $K-$parameter. The real $K-$parameter is associated with the phase front wreathed by a net of integer-charged vortices at the initial $z = 0$ plane. For example, when propagating, the vortices with $p = 1/2$ begin to form a group in such a way that the vortex net vanishes. There appears the smooth wave front looking like the helix with the phase shift $\Delta\Phi = \pi$ and the C-shaped intensity distribution. For the imaginary value of the $K-$parameter, the process evolves in the opposite direction [17]. Consider such a process in details.

B. Half integer-order vortices beams

The fractional-order vortex beams permit us to construct unusual wave structures with the broken axial symmetry. In contrast to the usual axial symmetric TE and TM modes with a local linear polarization in each point of the beam, the broken symmetry of the TE and TM mode beams with a fractional order $p=\pm 1/2$ vortices in each polarized component contains local elliptic polarizations at different points of the beam cross-section under the conditions $E_z=0$ for TE and $H_z=0$ for TM beams along the beam length. The broken symmetry of the vector field dictates the choice of the basis in the form of circularly polarized components.

From the equations (2) we obtain for the TE mode ($E_z=0,\ A_z=0$)

$$\partial_x E_x=-\partial_y E_y \text{ or } \partial_x A_x=-\partial_y A_y \tag{11}$$

and

$$\partial_x H_x=-\partial_y H_y \text{ or } \partial_x A_y=-\partial_y A_x \tag{12}$$

for the TM mode $\left(H_z=0,\ A_z=0\right)$.

It is convenient to employ the circularly polarized basis

$$A_+=A_x-iA_y,\quad A_-=A_x+iA_y \tag{13}$$

and a beam vortex structure needs new complex coordinates

$$u=x+iy=r\,e^{-i\varphi},\quad v=x-iy=r\,e^{i\varphi} \tag{14}$$

so that

$$\begin{aligned}\partial_u&=\partial_x-i\partial_y=\frac{e^{-i\varphi}}{2}\left(\partial_r-\frac{i}{r}\partial_\varphi\right),\\ \partial_v&=\partial_x+i\partial_y=\frac{e^{i\varphi}}{2}\left(\partial_r+\frac{i}{r}\partial_\varphi\right).\end{aligned} \tag{15}$$

Then we find for TE modes $A_+=\partial_u\Psi_p$, $A_-=-\partial_v\Psi_p$ or

$$\begin{aligned}E_+&=N\left[\partial_u F_p+i\,k\frac{v}{2Z}F_p\right]G,\\ E_-&=-N\left[\partial_v F_p+i\,k\frac{u}{2Z}F_p\right]G,\end{aligned} \tag{16}$$

where the function F_p obeys eq.(7).

In optical paraxial cases, where $\left|\partial_{u,v}F_p\right|<<k\left|F_p\right|$, we can use the approximation

$$E_+\approx iN\,k\frac{v}{2Z}F_pG,\quad E_+\approx -iN\,k\frac{u}{2Z}F_pG. \tag{17}$$

Similarly we obtain TM mode beams

$$E_{+} \approx iN\,k\frac{v}{2Z}F_{p}G,\quad E_{+} \approx iN\,k\frac{u}{2Z}F_{p}G. \tag{18}$$

Half-order $(2n+1)/2-$vortex-beams occupy a special place among variety of the fractional-charged optical fields because they can be easily and reliably generated at the initial plane by q-plates [23], photonic crystals [24] and arrays of microchip lasers [25]. Special types of singular beams with the fractional topological charges and fractional orbital angular momentum (OAM) in the closed form (e.g, erf-G beams and others) have been recently considered in number of papers [17, 18, 21, 26].

In this sub-section we will obtain the general closed form of the half-order vortex beams.

As a basic point we take the equation (7) and rewrite it in the form of

$$F_{p}(R,\varphi) = Ke^{i\frac{2n+1}{2}\varphi}\int_{-\varphi/2}^{\pi-\varphi/2} \mathrm{e}^{i(2n+1)\phi}\,\mathrm{e}^{-iKR\mathrm{os}2\phi}\,d\phi. \tag{19}$$

Remember that

$$\begin{aligned}
&\cos(2n+1)\phi\,d\phi = \sum_{j=0}^{[n+1/2]}(-1)^{j}C_{n}^{2j}\sin^{2j}\phi\cos^{n-2j}\phi = \\
&= \sum_{j=0}^{[n+1/2]}\sum_{m=0}^{n-j}(-1)^{n-j}C_{2n+1}^{2j}C_{n-j}^{m}\sin^{2(j+m)}\phi\;\; d(\sin\phi), \\
&\sin(2n+1)\phi\,d\phi = \sum_{j=0}^{n}(-1)^{j}C_{2n+1}^{j}\sin^{2j+1}\phi\cos^{2(n-j)}\phi = \\
&= -\sum_{j=0}^{n}\sum_{m=0}^{2j}(-1)^{m+j}C_{2n+1}^{j}C_{2j}^{m}\cos^{2(n-j+m)}\phi\;\; d(\cos\phi),
\end{aligned} \tag{20}$$

$C_{n}^{m}-$ a binomial coefficient.

For example,

$$\begin{aligned}
&\cos 3\phi = \left(1-4\sin^{2}\phi\right)d(\sin\phi), \\
&\sin 3\phi = -\left(4\cos^{2}\phi-1\right)d(\cos\phi).
\end{aligned} \tag{21}$$

After substituting (20) into (19) and integrating [22] we obtain

$$F_{p} = F_{n} = Ke^{i\frac{2n+1}{2}\varphi}\left\{\sum_{j=0}^{[n+1/2]}\sum_{m=0}^{n-j}(-1)^{n+j}C_{2n+1}^{2j}C_{n-j}^{m}F_{m,j}^{(s)} + \sum_{j=0}^{n}\sum_{m=0}^{2j}(-1)^{m+j}C_{2n+1}^{j}C_{2j}^{m}F_{m,j}^{(c)}\right\}, \tag{22}$$

where

$$
\begin{aligned}
F_{j,m}^{(s)} &= \frac{\Gamma\left(j+m+\frac{1}{2}\right)-\Gamma\left(j+m+1/2,\,-2iKR\sin^2\frac{\varphi}{2}\right)}{\left(-2iKR\right)^{1/2+j+m}},\\
F_{j,m}^{(c)} &= -\frac{\Gamma\left(j+m+\frac{1}{2}\right)-\Gamma\left(j+m+1/2,\,2iKR\cos^2\frac{\varphi}{2}\right)}{\left(2iKR\right)^{1/2+j+m}},
\end{aligned}
\tag{23}
$$

$\Gamma(n,x)$ stands for the incomplete Gamma function.

For example, the fractional beam with $p=3/2$ is described by the expression

$$
\begin{aligned}
\Psi_{3/2} &= \frac{NG}{\sigma}K\left\{F_{3/2}^{(s)}+iF_{3/2}^{(c)}\right\}e^{i\frac{3}{2}\varphi},\\
F_{3/2}^{(s)} &= -\left\{4\sqrt{\Re}\sin\frac{\varphi}{2}e^{-\Re\sin^2\frac{\varphi}{2}}+\sqrt{\pi}\left(\Re-2\right)erf\left(\sqrt{\Re}\sin\frac{\varphi}{2}\right)\right\}/\sqrt{\Re},\\
F_{3/2}^{(c)} &= \left\{4\sqrt{-\Re}\cos\frac{\varphi}{2}e^{-\Re\cos^2\frac{\varphi}{2}}-\sqrt{\pi}\left(\Re+2\right)erf\left(\sqrt{-\Re}\cos\frac{\varphi}{2}\right)\right\}/\sqrt{-\Re},\\
\Re &= 2iKR.
\end{aligned}
\tag{24}
$$

It is useful to mark that the function $\Psi_{3/2}$ in eq. (24) is a periodic one with the period 2π despite the factors $\cos\frac{\varphi}{2}$ and $\sin\frac{\varphi}{2}$ in the functions $F_{3/2}^{(c,s)}$. In order to prove it, it is necessary to take into account the factor $e^{i\frac{3}{2}\varphi}$ in the function $\Psi_{3/2}$ and oddness of the function $erf(x)$.

The presented above results are of a new family of asymmetric scalar vortex beams with $p=\pm(2n+1)/2$ that we call Gamma-Gaussian beams ($\Gamma-G$ beams) referring to the complex amplitude Ψ_p. The $\Gamma-G$ beams are a natural generalization of the $erf-G$ beams [17] over all set of half integer-order vortex topological charges.

Typical representatives of the $\Gamma-G$ family of the singular beams are shown in Fig. 1. Thus, the field distributions at the beam cross-section depend essentially on the value of the $K-$ parameter. When the $K-$ parameter has a pure real value (Fig. 1) the intensity distribution has a $C-$ like profile at $z=0$ with the only half-integer order vortices near the center (see e.g. [17]).

However, when propagating the intensity profile is drastically transformed turning into broken Bessel beam at the length $z >> z_0$ with integer-order vortices scattering over the beam cross-section. For the pure imaginary $K-$ parameter ($|K|$ is constant), the process is reversed.

The phase distributions shown in Fig. 1 (b) illustrate a complex phase structure for different half-order vortex topological charges.

A smooth growth of the phase up to $\Phi = \pi / 2$ for $p = 1/2$ is replaced by the phase oscillations in the broken second branch of the two-leaved helicoid for the topological charge $p = 3/2$. The phase loss is $\Delta\Phi = \pi / 2$. The same phase construction is observed for the topological charge $p = 5/2$ where the third branch of the three-leaved helicoid lacks also the phase $\Delta\Phi = \pi / 2$. All phase losses are accompanied by smooth variations. The sign alternation $p \to -p$ changes the direction of the helicoid twist.

All the above equations enable us to build a great number of asymmetric transverse electric TE and transverse magnetic *TM* beams. Some of them are shown in Fig. 2.

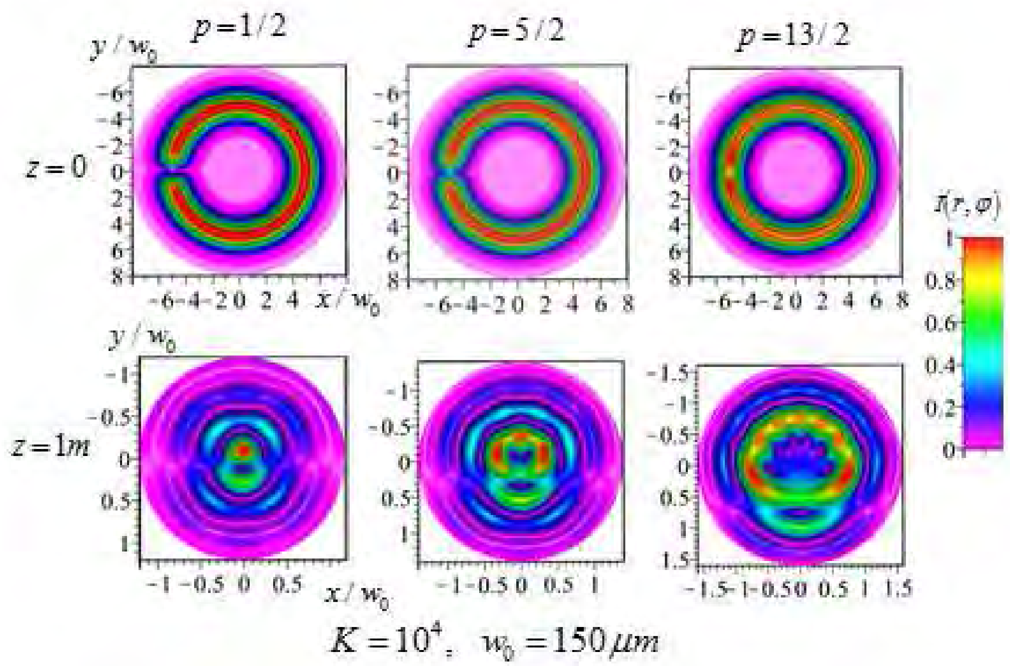

Fig. 1. (a) Intensity distributions of the Gamma-Gaussian ($G-\Gamma$) beams with different topological charges p at the initial plane and at the far diffraction zone

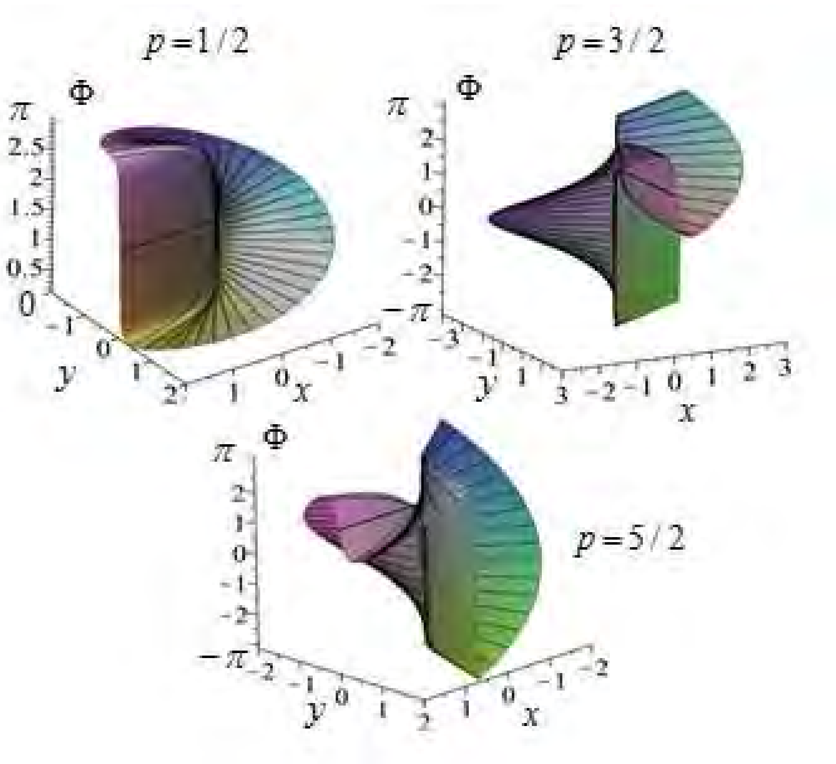

Fig. 1. (b). Phase distributions $\Phi(r,\varphi)$ at the initial plane $z=0$

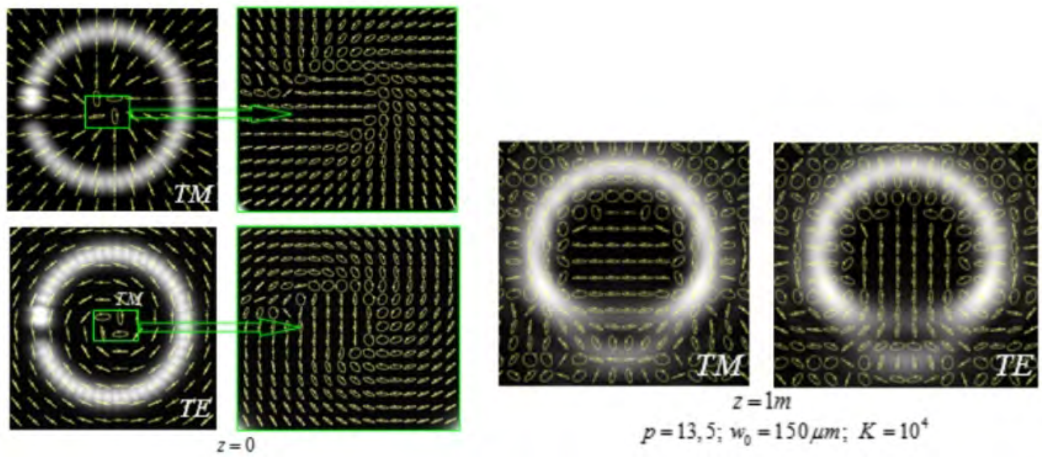

Fig. 2. The field distributions of the $\Gamma-G$ beams for different topological charges at the background of the intensity distributions

The fine structure of these fields is reshaped along the beam length, so that the beams are structurally unstable under propagation in free space. In contrast to standard TE and TM modes the asymmetric paraxial beam fields in Fig. 2 are elliptically polarized at each point of the beam cross-section with distinctive orientations of the ellipse axes. Near the optical axis, the field tends to form two polarization singularities of a kind (the star or lemon [12]). Far from the center, the directions of the linear polarization are wound into Archimedean (for TE) and logarithmic (for TM) spirals.

The peculiar feature of the $\Gamma-G$ beams is also their capacity to gather together integer-order vortices into one with the fractional topological charge at far diffraction zone when the $K-$ parameter is a pure real value while a pure imaginary value of the $K-$ parameter induces the reverse process – the fractional vortex decays into an infinite number of integer-order vortices. Such beam behavior reflects the inherent processes in the fractional-order vortex structures in contrast to the representation of the inevitable vortex decaying.

In essence, all types of the considered above fractional order beams are the structurally unstable under propagation.

C. Shaping the integer-order vortex beams

Can the fractional-order vortex beams form a stable state of the singular beam with the centered integer-order vortex? This a key question of our consideration here.

At first, we will analyze a dipole structure consisting of two orthogonal states $\left|p\right\rangle$ and $\left|-p\right\rangle$:

$$\left|p,-p\right\rangle=\left|p\right\rangle+\left|-p\right\rangle=Q\sum_{m=-\infty}^{\infty}\frac{i^m m\, e^{im\varphi}}{p^2-m^2}J_m\left(KR\right), \tag{25}$$

where $Q=2N\,G\left(r,z\right)\sin\left(\pi p\right)\,e^{i\pi p}$. The state (25) we can regard as the initial topological dipole.

After rotating the initial dipole through an angle $\varphi_q=\dfrac{\pi}{q}$ (Fig. 3) so that $\varphi\to\varphi+\dfrac{\pi}{q}$ we obtain

$$\left|p,-p,q\right\rangle=Q\sum_{m=-\infty}^{\infty}\frac{i^m m\, e^{im\varphi}}{p^2-m^2}J_m\left(KR\right)e^{im\frac{\pi}{q}}. \tag{26}$$

Superposition of the equations (25) and (26) gives a new dipole

$$|\,p,-p,\pm\rangle = |\,p,-p\rangle + |\,p,-p,q\rangle = \\ = Q\sum_{m=-\infty}^{\infty}\frac{i^m m\, e^{im\varphi}}{p^2-m^2}J_m\left(KR\right)\left(1\pm e^{im\frac{\pi}{q}}\right). \tag{27}$$

If $q=1$ the terms with $m=2m'+1$ for a sign $(+)$ vanish while the residual terms forming the state

$$|\,p,2,+\rangle = i4Q\sum_{m=0}^{\infty}(-1)^m\frac{(2m)\sin(2m\varphi)}{p^2-(2m)^2}J_{2m}(KR). \tag{28}$$

In turn, for a sign $(-)$, the terms with $m=2m'$ vanish and we find the state

$$|\,p,2,-\rangle = -4Q\sum_{m=0}^{\infty}(-1)^m\frac{\left[(2m+1)\right]\sin\left[(2m+1)\varphi\right]}{p^2-\left[(2m+1)\right]^2}J_{2m+1}(KR). \tag{29}$$

The first state (28) does not contain any optical vortices but only the set of edge dislocations of the order $p=2$ as well as the equation (29) with $p=1$.

In order to obtain hight-order beams, e.g. with $p=4$, we set a phase difference between two dipole states (30) equal to $\Delta\varphi_n=\pi$. As a result one obtains

$$|\,p,4,\pm\rangle = Q\sum_{m=-\infty}^{\infty}(-1)^m\frac{(2m)e^{i2m\varphi}(1\pm e^{im\pi})}{p^2-(2m)^2}J_{2m}(KR) \tag{30}$$

so that the two states are

$$|\,p,4,+\rangle = i2Q\sum_{m=0}^{\infty}(-1)^m\frac{(4m)\sin(4m\varphi)}{p^2-(4m)^2}J_{4m}(KR) \tag{31}$$

for the sign $(+)$, and

$$|\,p,4,+\rangle = i2Q\sum_{m=0}^{\infty}(-1)^m\frac{(4m+2)\sin(4m+2)\varphi}{p^2-(4m+2)^2}J_{4m}(KR). \tag{32}$$

for the sign $(-)$

By means of such a recurring procedure one finds the general expressions

$$|\,p,2s\rangle = i2Q\sum_{m=0}^{\infty}(-1)^m\frac{(4s\,m)\sin(4s\,m\varphi)}{p^2-(4sm)^2}J_{4sm}(KR),\ s=1,2,...,, \tag{33}$$

$$|\,p,2s+1\rangle = -2Q\sum_{m=0}^{\infty}(-1)^m\left[2s(2m+1)+1\right]\frac{\sin\left[2s(2m+1)+1\right]\varphi}{p^2-\left[2s(2m+1)+1\right]^2}J_{2s(2m+1)+1}(KR), \quad (34)$$

$s=0,1,2....$

where s is a number of the recurring transformations, whereas $2s$ and $2s+1$ are topological indices of the wave constructions.

The following step is to rotate the initial dipole through an angle $\varphi_0=\dfrac{\pi}{2}$. Such a transformation turns sine in (33) and (34) into cosine at $m=0$ at arbitrary index s. As a result we obtain the states with the centered optical vortices of the required integer-order topological charges $l=2s$ or $l=2s+1$

$$|\,p,\pm l\rangle = |\,p,s\rangle_0 \pm i\,|\,p,s\rangle_{\pi/2}. \quad (35)$$

Intensity distributions of the axially symmetric fields shown in Fig. 3a, c illustrate the optical constructions built up of the broken fractional vortex-beams on the base of the expressions (33) and (34).

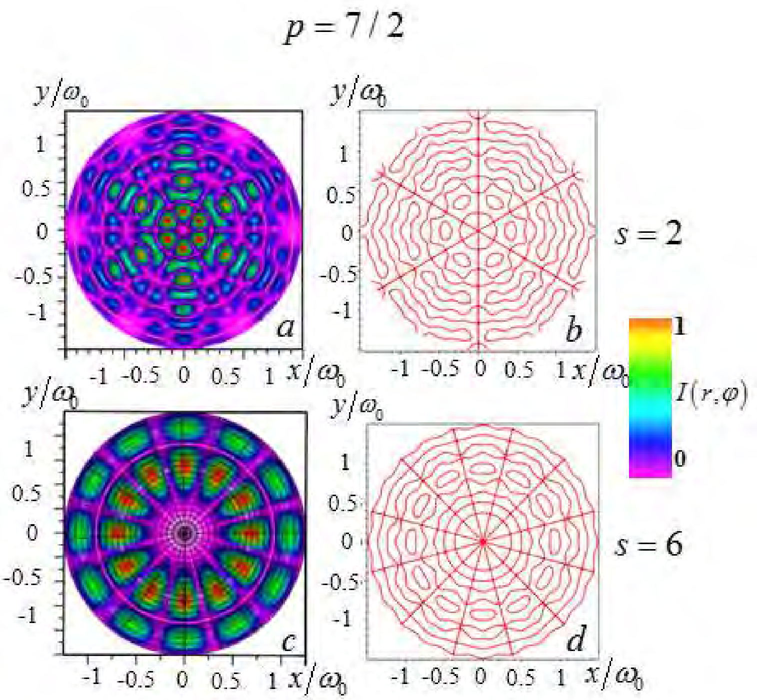

Fig. 3. Intensity distributions and L-lines of the axially symmetric beams shaped by the fractional-order vortex beams

Astonishing feature of these structures is that there are no optical vortices in them. Instead we see in Fig. 3b, d the curlie-wurlie of the degenerated edge dislocations (L-lines [48]) webbing tightly around the beam pattern. Three (Fig. 3 b) and six (Fig. 3 d) nodal lines intersect each other at the axis.

As a result, expressions (35) and (36) are responsible for shaping the optical tracery shown in Fig. 4 consisting of the interchangeable arranged vortex arrays and degenerated edge dislocations around the centered optical vortex with the topological charges $l=3$ and $l=6$.

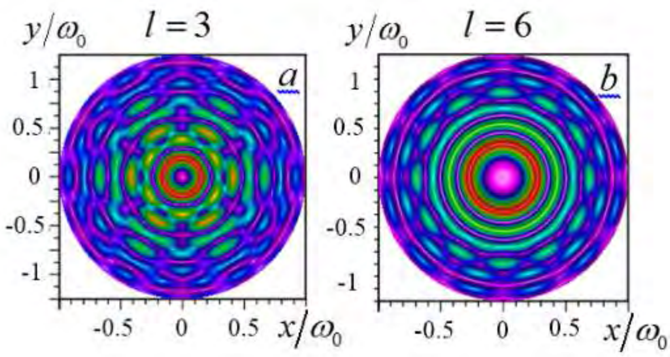

Fig. 4. Intensity beam distributions with centered higher-order vortices and complex vortex framing

Thus, a simple rotation of two topological dipoles through discrete angles (Fig. 5) enables us to form singular beams with the required, centered integer-order optical vortices.

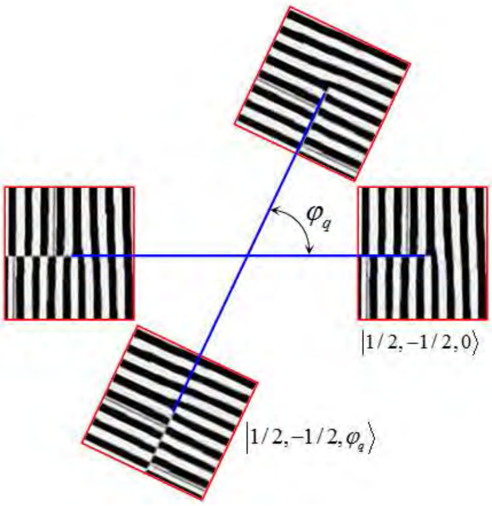

Fig. 5. The sketch of the topological dipole and its angular rotation

When propagating such a complex beam transforms it's framing far from the axis while the central part preserves the singular structure.

At the same time, all the beam states (both with the integer-order and fractional-order vortices) in free space or uniform isotropic media are degenerated, i.e. have the same propagation constants independent on the topological charge values. The choice of the beam representation in one or other basis is determined by the intrinsic symmetry of the optical system. Despite the fractional vortex beam degeneracy in free space, the results presented above enable us to originate new vortex-beam constructions that can open their extraordinary properties in non-uniform anisotropic media as we will see it later.

Also, the problem of the "hidden phase" of the fractional-order vortices [4] in the circularly polarized field components slipped out from our consideration since the fractional-order vortex, as a rule, decays into an infinite number of the integer-order vortices under propagation.

However, the exclusion is the $\Gamma - G$ beams that can either break down the fractional vortex into a set of integer-order vortices or, vice-versa, gather them together into one fractional vortex at far diffraction zone. The control for these counter-directed processes brings into effect the modulation of the beam parameter K.

Further we consider two examples of the possible manifestations of the fractional-order vortex beams in the uniform and non-uniform anisotropic media with the distinctive intrinsic symmetry.

2. DECAY OF OPTICAL QUARKS IN UNIAXIAL IN BIAXIAL CRYSTALS

A. General remarks

The fractional-charged beams propagating in uniaxial crystals has been partially regarded in [26] for the vortex beams in states $\left|\pm 1/2\right\rangle$ (the so-called erf-G beams). Authors showed conversion between the states $\left|\pm 1/2\right\rangle$ $\left|1/2 \pm 2\right\rangle$ in circular polarized components. It is easily to generalize this rule to arbitrary states $\left|p\right\rangle$ $\left|p \pm 2\right\rangle$. However all the states with different fractional-order vortices are degenerated.

Alternatively, biaxial crystals have one interesting type of the dielectric tensor singularity – Hamilton's diabolical point [28] that defines particular behavior of the vortex beams propagating along one of the crystal optical axes – so called the conical refraction predicted by Hamilton due to a peculiar space-variant birefringence (see Fig. 6).

The internal conical refraction is in spreading a narrow light beam propagating along the crystal optical axis into a hollow cone [29]. The initial circular polarization of the beam splits into a cone of local linear polarizations in such a way that the electric vector $\mathbf{E}$ rotates though an angle π after a full path tracing around the cone axis as shown in Fig. 6. Generalization of Hamilton`s approach onto Gaussian beams introduces corrections into a fine structure of the field propagation and distribution [28]. The phenomenon is called the conical diffraction. The conical form of the beam suggested the solutions of the problem in the form of Bessel beams. At the same time, the polarization distribution in Fig.6 has also much in common with that of $erf - G$ and $\Gamma - G$ beams in Fig. 4 [17].

Little misalignments of the field patterns far from the optical axis can be referred to a complex structure of the fractional-charged vortex beams.

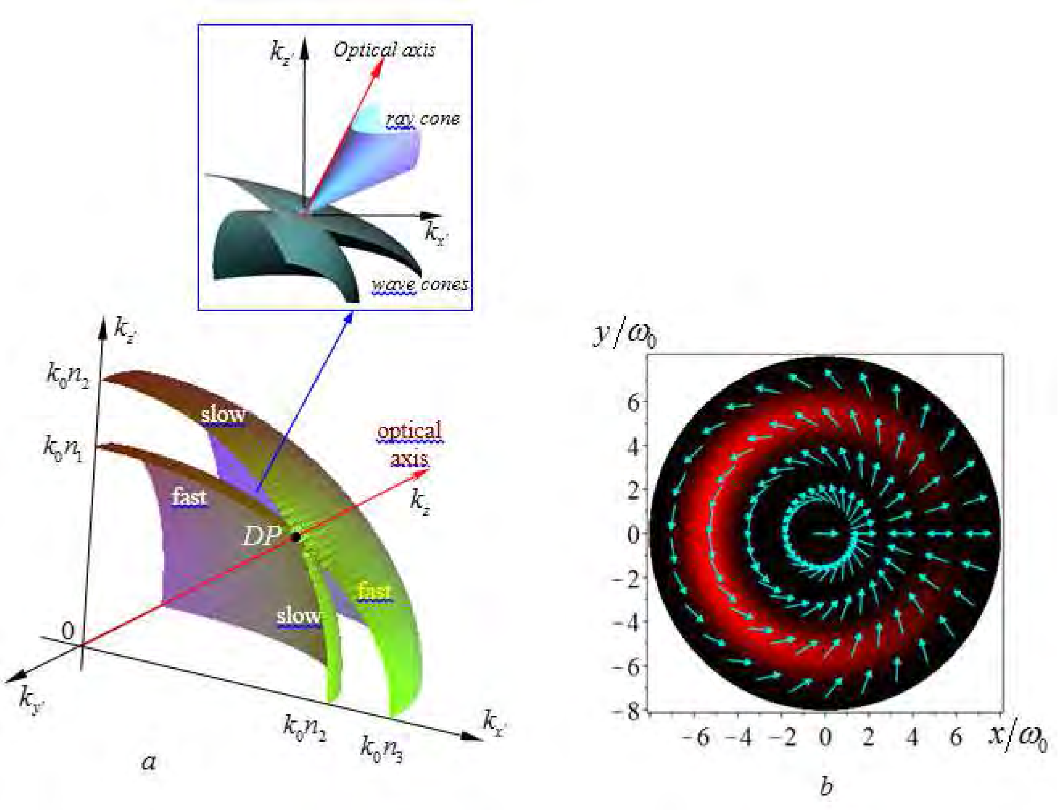

Fig. 6. (a) The shaping of a diabolic point (DP) in a biaxial crystal as intersection of two wave surfaces. The *callout illustrates* places of the ray and wave cones of the conical refraction; (b) Space-variant directions of the biaxial crystal birefringence under the conditions of the conical refraction on the background of the beam intensity

The unexpected results presented in the papers [29, 30, 31, 32] have shown that the uniaxial crystal exhibits a tendency to turn into a biaxial one after twisting it around the optical axis. The space-variant symmetric field of TE or TM eigen modes inherent to a uniaxial crystal [33] at the initial plane $z=0$ transforms into the asymmetric field distribution similar to that shown in Fig. 6. In contrast to the standard conical diffraction in the typical biaxial crystals, the intensity distribution in the twisted uniaxial crystal has not the pronounced C-shaped form or the circular form with Poggendorff rings [29] but the pattern gets smeared over the cross-section with the singular point at the axis. Nevertheless, the fine structure of the pattern can be controlled by means of either mechanical or electrical devices.

The presented results point out on the fact that eigen mode beams of the conical diffraction and adjoining phenomena are worth searching among the fractional-order vortex-beams.

Thus, the aim of the following sub-section is to study the propagation and conversion of the fractional-order vortex-beams of the Bessel type along one of the optical axes of the biaxial crystal. We will focus our attention to the question: could the input beam field with a space variant polarization identical to that of the crystal birefringence (say, the state $|p\rangle$) propagate without structural perturbation (to be the propagation-invariant wave constructions)? If yes, then we can expect the fractional-order mode beam to be an eigen mode of the medium.

B. The theoretical treatment

The underlying idea of our treatment leans on the constitutive papers [34–37] where authors consider evolution of the electric field $\mathbf{E}$ (rather than the electric displacement $\mathbf{D}$) of Bessel beams in biaxial crystals under the condition of conical diffraction. The fact is that the wave normal is not directed along the beam propagation in a biaxial crystal so that there appear additional terms in the vector wave equation because of changes in the permittivity tensor. In our case we can use this tensor in the form [37]

$$\hat{\varepsilon} = \begin{pmatrix} \varepsilon_a & 0 & -\varepsilon_{13} \\ 0 & \varepsilon_2 & 0 \\ -\varepsilon_{13} & 0 & \varepsilon_b \end{pmatrix}, \tag{36}$$

where $\varepsilon_a = \varepsilon_1 + \varepsilon_3 - \varepsilon_1\varepsilon_3 / \varepsilon_2$, $\varepsilon_b = \varepsilon_1\varepsilon_3 / \varepsilon_2$, $\varepsilon_{13} = \sqrt{\varepsilon_1\varepsilon_3\left(\varepsilon_2 - \varepsilon_1\right)\left(\varepsilon_3 - \varepsilon_2\right)} / \varepsilon_2$, $n_1^2 = \varepsilon_1$, $n_2^2 = \varepsilon_2$, $n_3^2 = \varepsilon_3$ are the principal refractive indices of the crystal along the axes x', y', z'.

The optical axis directed at the angle θ to the axis z'

$$\tan\theta = \sqrt{\frac{\varepsilon_3\left(\varepsilon_2 - \varepsilon_1\right)}{\varepsilon_1\left(\varepsilon_3 - \varepsilon_2\right)}}. \quad \varepsilon_1 < \varepsilon_2 < \varepsilon_3$$

passes through a diabolic point where slow (s) and fast (f) wave fronts are tangent to each other as shown in Fig. 7.

Author of the papers [35, 38] showed that the circularly polarized beam components with the spectral function at the crystal input $A\left(k_\perp\right)$ ($k_\perp$ is the transverse wavenumber of the initial beam), are

$$E_{+}(r,\varphi,z)=\sum_{m'=-\infty}^{\infty} e^{im'\varphi}\int i^{m'} k_{\perp} A_{m'}(k_{\perp}) J_{m'}(k_{\perp} r)\exp\left(-i\frac{k_{\perp}^{2}}{2k_{b}}z\right)\cos(\gamma_{0}k_{\perp}z)\,dk_{\perp}e^{i\beta z},$$
$$E_{-}(r,\varphi,z)=-\sum_{m'=-\infty}^{\infty} i^{m'} e^{i(m'+1)\varphi}\int k_{\perp} A_{m'}(k_{\perp}) J_{m'+1}(k_{\perp} r)\exp\left(-i\frac{k_{\perp}^{2}}{2k_{b}}z\right)\sin(\gamma_{0}k_{\perp}z)\,dk_{\perp}e^{i\beta z}.$$
(37)

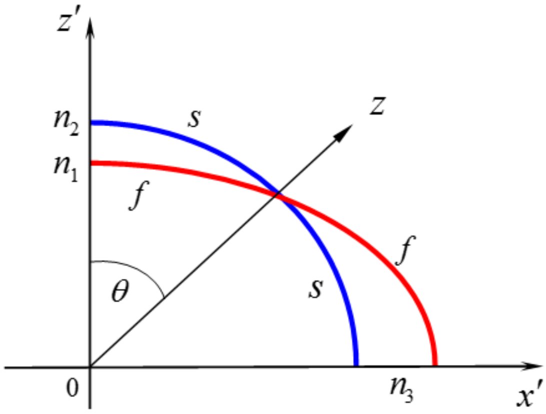

Fig. 7. Sketch of the surface of normals of the slow (s) and fast wavefronts and the optical axis direction

It means that the right-hand circularly polarized beam bearing a series of the vortex-beams of the m-order and a complex angular spectral distribution $A(k_{\perp})$ at the crystal input stimulates an excitation of a series of the vortex-beams of the m+1 – order with the same angular spectrum $A(k_{\perp})$ in the left-hand circularly polarized component.

Similarly, it can be shown that the composition of the vortex beams of the m+1 – order with the spectral distribution $A(k_{\perp})$ in the left circularly polarized component at the crystal input excites a series of a series of the vortex-beams of the m – order with the same angular spectrum $A(k_{\perp})$ in the right-hand circularly polarized component, i.e.

$$E_{+}(r,\varphi,z)=\sum_{m'=-\infty}^{\infty} e^{im'\varphi} i^{m'}\int k_{\perp} A_{m'}(k_{\perp}) J_{m'}(k_{\perp} r)\exp\left(-i\frac{k_{\perp}^{2}}{2k_{b}}z\right)\sin(\gamma_{0}k_{\perp}z)\,dk_{\perp}e^{i\beta z},$$
$$E_{-}(r,\varphi,z)=\sum_{m'=-\infty}^{\infty} i^{m'} e^{i(m'+1)\varphi}\int k_{\perp} A_{m'}(k_{\perp}) J_{m'+1}(k_{\perp} r)\exp\left(-i\frac{k_{\perp}^{2}}{2k_{b}}z\right)\cos(\gamma_{0}k_{\perp}z)\,dk_{\perp}e^{i\beta z}.$$
(38)

The circularly polarized single Bessel beam $E_+^{in} = J_m\left(k_\perp r\right)\exp\left(im\varphi\right)e^{ik_z z}$ with integer-order topological charge m, directed along the crystal optical axis (axis z in Fig. 7), has the conical spectral distribution $A\left(k_\perp = k_\perp^{(0)}\right) = const$. In order to obtain the beam propagation of such a beam it is sufficient to multiply eq. (37) by the factor $\delta\left(k_\perp - k_\perp^{(0)}\right)$, and taking into account $m' \to m$ we find

$$\mathbf{E}_1 = \begin{pmatrix} E_+ \\ E_- \end{pmatrix} = \begin{pmatrix} J_m\left(k_\perp r\right)\exp\left(im\varphi\right)\cos\left(\gamma_0 k_\perp z\right) \\ -J_{m+1}\left(k_\perp r\right)\exp\left[i\left(m+1\right)\varphi\right]\sin\left(\gamma_0 k_\perp z\right) \end{pmatrix}\exp\left(-i\frac{k_\perp^2}{2k_b}z\right)e^{i\beta z}, \tag{39}$$

where $\beta = n_2 z,\ k_b = k\, n_2 / 2\left(1+\varepsilon_2/\varepsilon_b\right),\ \gamma_0 = \varepsilon_{13}/2\varepsilon_b.$

Similar to that we can obtain from eq. (38) for the initial field in the form $E_-^{in} = -J_{m+1}\left(k_\perp r\right)\exp\left[i\left(m+1\right)\varphi\right]e^{ik_z z}$ the expression

$$\mathbf{E}_2 = \begin{pmatrix} E_+ \\ E_- \end{pmatrix} = \begin{pmatrix} J_m\left(k_\perp r\right)\exp\left(im\varphi\right)\sin\left(\gamma_0 k_\perp z\right) \\ J_{m+1}\left(k_\perp r\right)\exp\left[i\left(m+1\right)\varphi\right]\cos\left(\gamma_0 k_\perp z\right) \end{pmatrix}\exp\left(-i\frac{k_\perp^2}{2k_b}z\right)e^{i\beta z}. \tag{40}$$

Combination $\mathbf{E}_1 \pm i\mathbf{E}_2$ of (39) and (40) gives

$$\mathbf{E} = \frac{1}{2}\begin{pmatrix} J_m\left(k_\perp r\right)\exp\left(im\varphi\right) \\ J_{m+1}\left(k_\perp r\right)\exp\left[i\left(m+1\right)\varphi - i\frac{\pi}{2}\right] \end{pmatrix}\mathrm{e}^{i\left(\frac{k_\perp^2}{2k_b}+\gamma_0 k_\perp+\beta\right)z} \tag{41}$$

and

$$\mathbf{E} = \frac{1}{2}\begin{pmatrix} J_m\left(k_\perp r\right)\exp\left(im\varphi\right) \\ J_{m+1}\left(k_\perp r\right)\exp\left[i\left(m+1\right)\varphi + \frac{\pi}{2}\right] \end{pmatrix}\mathrm{e}^{i\left(\frac{k_\perp^2}{2k_b}-\gamma_0 k_\perp+\beta\right)z} \tag{42}$$

The equations (41) and (42) show that such fields with space-variant polarization can propagates through the crystal without any structural transformations but with different propagation constants $\beta_\pm = \frac{k_\perp^2}{2k_b} \pm \gamma_0 k_\perp + \beta$.

Difference between the propagation constants $\beta_\pm$ of the mode beams is connected with rotation of the mode fields $\mathbf{E}_1$ and $\mathbf{E}_2$ through an angle π. Fig. 6 demonstrates the situation when the local directions of the space-variant birefringence $\Delta n\left(\varphi\right)$ of the crystal coincides with the local directions of the local field distribution that corresponds the propagation constant β_+. The field rotation at the angle $\varphi_0 = \pi$ results in changing the sign of the local birefringence $\Delta n(\varphi) \to -\Delta n(\varphi)$ that corresponds to replacement $\beta_+ \to \beta_-$.

The polarization state distribution of the s at the mode beam cross-section (6) has a complex form in contrast to the standard structure shown in Fig. 6. A typical space-variant polarization illustrates Fig. 8 for the mode index $m = 6$.

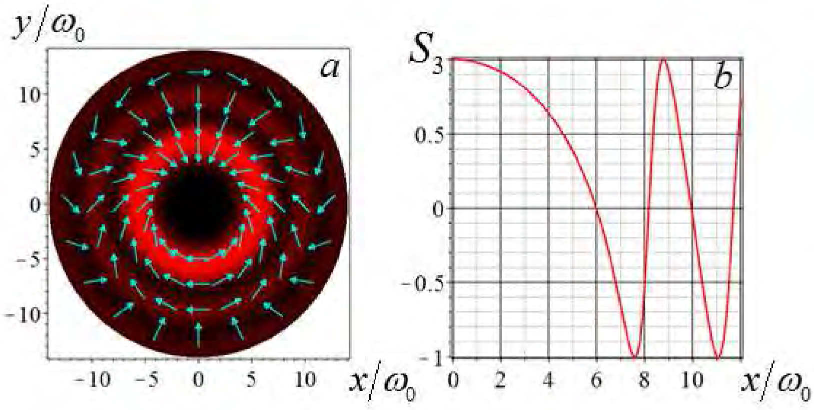

Fig. 8. The polarization state distribution of the mode beam with the index $m = 6$ (a) and (b) the dependence of the ellipticity degree $S_3(r)$ along the beam radius

Directions of the polarization ellipse axes ψ are depicted on the background of the mode intensity distribution. The ellipticity states specified by the Stokes parameter S_3 as a function of radial position in Fig. 8 b oscillate from the right-hand $S_3 = 1$ to left-hand $S_3 = -1$ states. However, the ellipticity S_3 preserves its value along the azimuth direction $\hat{\boldsymbol{\varphi}}$. Although the path-thracing around the beam axis through an angle $\varphi = \pi$ is accompanied by the ellipse rotation through an angle $\psi = \pi/2$, the full path-tracing results in reinstating both the polarization state and beam phase. Such a space-variant polarization of the eigen mode manifest itself in the ring pattern of intensity distribution while the linear space-variant polarization is in line with *C*-shaped distribution in Fig. 6.

The partial solutions (41) and (42) in the form of eigen modes can be extended to a general solution as a superposition of (41) or (42) with different values of indices m. In particular, the mode field $\mathbf{E}_p^{(+)}$ with the propagation constant β_+ and the fractional topological charge p in the right-hand component can be presented as

$$\mathbf{E}_p^{(+)} = c_p \begin{pmatrix} \sum_{m=-\infty}^{\infty} \dfrac{i^m J_m\left(k_\perp r\right)\exp\left(im\varphi\right)}{p-m} \\ -\sum_{m=-\infty}^{\infty} \dfrac{i^{m+1} J_{m+1}\left(k_\perp r\right)\exp\left[i\left(m+1\right)\varphi\right]}{p-m} \end{pmatrix} e^{i\beta_+ z} =$$

$$= c_p \begin{pmatrix} \sum_{m=-\infty}^{\infty} \dfrac{i^m J_m\left(k_\perp r\right)\exp\left(im\varphi\right)}{p-m} \\ -\sum_{m=-\infty}^{\infty} \dfrac{i^{m+1} J_{m+1}\left(k_\perp r\right)\exp\left[i\left(m+1\right)\varphi\right]}{p+1-\left(m+1\right)} \end{pmatrix} e^{i\beta_+ z} == \begin{pmatrix} |p\rangle \\ -c_{p+1}\left|p+1\right\rangle \end{pmatrix} \exp\left(-i\beta_+ z\right), \tag{43}$$

where $c_p = \sin\pi p \; e^{ip\pi}$. Similar to that we can write down the mode field $\mathbf{E}_p^{(-)}$ with the propagation constant β_-:

$$\mathbf{E}_p^{(-)} = \begin{pmatrix} |p\rangle \\ i\,c_{p+1}\left|p+1\right\rangle \end{pmatrix} \exp\left(-i\beta_- z\right), \tag{44}$$

with $\beta_\pm = \dfrac{k_\perp^2}{2k_b} \pm \gamma_{in} k_\perp - \beta$ and we employ the expression (44).

Typical field distributions on the background of the beam intensity is shown in Fig. 9 for the $\left|0.5\right\rangle$ and $\left|7.5\right\rangle$ fractional states.

We calculated the states for the potassium gadolinium tungstate KGd[WO$_4$]$_2$ (KGW) biaxial crystal with refractive indices $n_1 = 2.013, n_2 = 2,045, n_3 = 2.086$, for the wavelength $\lambda = 0.63\,\mu m$, so that the crystal and beam control parameters are $\gamma_{in} \approx 0.0087\,rad$, $\varepsilon_b \approx 4,224$, $k_\perp \approx 1.74\cdot 10^5 m^{-1}$. We found the beams in all beam states to have a linear polarization at the cross-section. In contrast to the integer-order vortex charges (see Fig. 8), an angle rotation of the liner polarization ψ of the fractional-order states is multiple to π after a full path-tracing around the axis and depends on both the topological charge p and a transverse position r. Besides, we found that the greater the value of the parameter $k_\perp$ the greater the number of polarization variations along the radial $\hat{\mathbf{r}}$ directions.

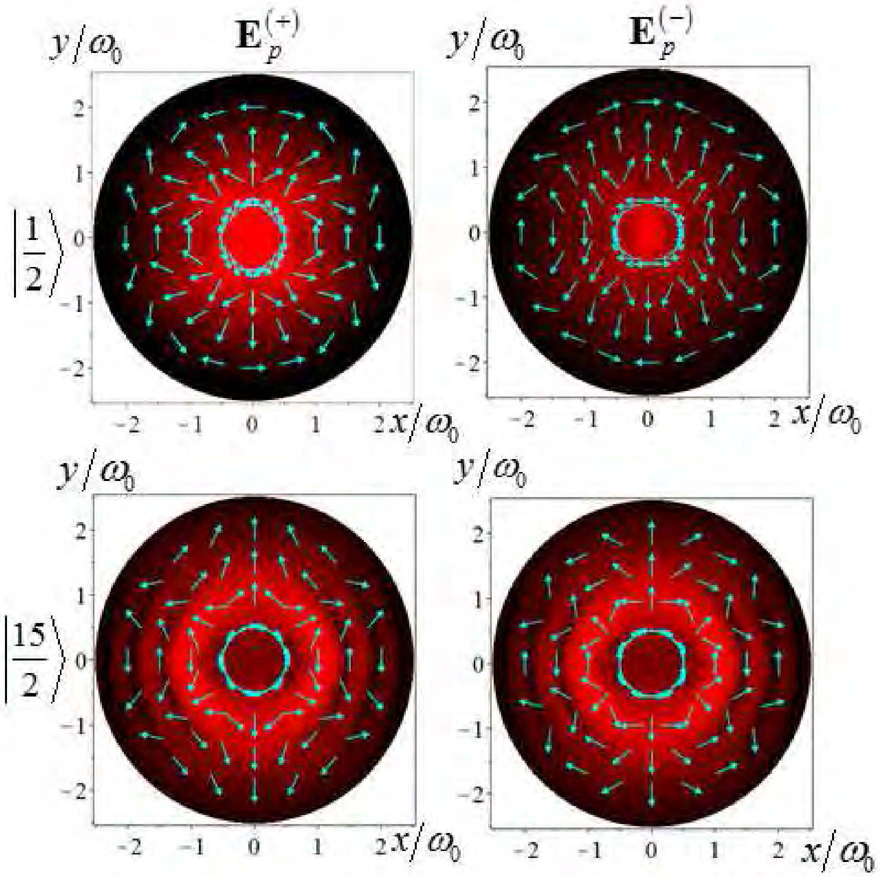

Fig. 9. Field distributions of the fractional-order vortex beam in the potassium gadolinium tungstate KGW biaxial crystal

The beat length in our case equals to $L_B = 2\pi/(\gamma_{in}k_\perp) \approx 4.15\,mm$. It means that the states $|p\rangle$ and $|p+1\rangle$ appear alternately at this length while the eigen mode states (43) and (44) in Fig. 9 emerge at the lengths $L_{e,o} = \pi(2n+1)/(4\gamma_{in}k_\perp), n = 0,1,2,....$

Thus, the right-hand circularly polarized Bessel beam with the $p-$ fractional-order vortex at the crystal input induces the beam with $p+1-$ fractional-order vortex at the left-hand circular polarization at some crystal length z. At the beam length $z = \dfrac{\pi}{2\gamma k_\perp}(2n+1)$, $n = 0,1,2,...$ all energy state is transported from $|p\rangle$ into $|p+1\rangle$ state. However the eigen modes $\mathbf{E}_p^{(\pm)}$ for different charges p have the same propagation constants (i.e. are degenerated). Any superposition of the fractional-order vortex beams obeys the same transformations (45) as the single field states.

Thus, the energy transport of the conical diffraction process in biaxial crystals is carried out from E_+ component in $|p\rangle$ state into E_- component in $|p+1\rangle$ state and vice-versa for wide types of the field structure of fractional-order vortex beams. However, difference of the propagation constants between the orthogonal field components is the same for all types of the fractional-order vortex-beams. There is not an appropriate physical mechanism in the biaxial crystals that could make the polarization structure of the beam to follow the singular structure with the fractional-order index of the birefringence directions. As a result the biaxial crystals cannot maintain the single fractional-order vortex beams without their decay into a set of the integer-order vortices.

Let us now peer more attentively into shaping the beam structure in space-variant birefringent media.

CONCLUSION

Different types of symmetry of optical media are the key points that specify properties of the singular beam propagation. It is such starting points that were the base of our consideration. At first, we have considered variety of vector fractional-order vortex beams that can be transmitted through free space or a uniform isotropic medium. Among them the Gamma-Gaussian beams (the $\Gamma-G$ beams, in particular, the erf-G beams) occupy a special place. The fact is that in contrast to the prevalent opinion about decaying the initial fractional-order vortex into a cloud of integer-order vortices, the $\Gamma-G$ beams either break apart of the fractional vortex or, vice-versa, gather together integer-order vortices into one fractional-order vortex at far diffractive zone. However, all types of such vortex beams are unstable under propagation.

On the other hand, we revealed that singular beams with the stable centered integer-order vortices can be formed by four fractional-order vortices. Such constructions remains stable for different values of the topological charges p.

We found that the space-variant birefringence with one singular point shown in Fig.6 is inherent in the fractional-order vortex-beams at the crystals input under the condition of the conical diffraction. Typical scenario of the beam propagation here evolves in such a way that the topological charges of the fractional-order vortices in the circularly polarized components of vector beams differ from each other in one unit. The difference between the propagation constants of the components is independent on the value p. It means that the biaxial crystal does not feel distinction between the fractional- and integer-order vortex beams. The same processes we observe also in the so-called *q*-plates, Moreover the polarization states at the beam cross-section are distributed by the complex way far from that of the birefringent directions in the crystal. Naturally the fractional-order vortex beams in the biaxial crystals and q-plates are also unstable one under propagation.

References

1. M. S. Soskin and M. V. Vasnetsov, *Prog. Opt.* **42**, 219 (2001).
2. I. Basisty, M. Soskin, M. Vasnetsov, *Opt. Commun.* **119**, 604 (1995).
3. I. Basisty, et al., *J. Opt. A-Pure Appl. Op.* **6**, S166 (2004).
4. M. V. Berry et al., *Eur. J. Phys.* **1**, 154 (1980).

5. M. V. Berry, *J. Opt. A –Pure Appl. Op.* **6**, 259 (2004).
6. G. E. Volovik and V. P. Mineev, *Pis'ma Zh. Eksp. Teor. Fiz.* **24**, 605 (1976).
7. J. Jang et al., *Science* **331**, 186 (2011).
8. S. W. Seo, S. Kang, W. J. Kwon, and Yong-il Shin, *Phys. Rev. Lett.* **115**, 051301 (2015).
9. J. A. Sauls, *Physics* **9**, 148 (2016).
10. A. Hansen, J. T. Schuliz, N. P. Bigelow, *Optica* **3,** 355 (2016).
11. S. Tao, W. Lee, X. Yuan, *Appl. Opt.* **43**, 122 (2004).
12. J. Leach, E. Yao, and M. J. Padgett, *New J. Phys.* **6**, 71 (2004).
13. H. Garcia, J. Gutierrez-Vega, *J. Opt. Soc. Am. A* **26**, 794 (2009).
14. J. C. Gutiérrez-Vega and C. López-Mariscal, *J. Opt. Soc. Am. A* **10**, 015009 (2008).
15. F. G. Mitri, *Opt. Lett.* **36**, 606–608 (2011).
16. Yiqi Fang et al., *Phys. Rev. A* **95**, 023821 (2017).
17. T. A. Fadeyeva et al., *Opt. Lett.* **37**, 1397 (2012).
18. T. A. Fadeyeva, A. F. Rubass, R. V. Aleksandrov, A. V. Volyar, *J. Opt. Soc. Am. B* **31**, 798 (2014).
19. G. Maleshkov, D. Neshev, A. Dreischuh, *Phys. Rev. A* **80**, 053828 (2009).
20. C. Alexeyev et al., *Opt. Lett.* 42, **4**, 783 (2017).
21. A. P. Kiselev, *Opt. Spectrosc.* **96**, 479 (2004).
22. F. Cardano, E. Karimi, S. Slussarenko, L. Marrucci, Corrado de Lisio, E. Santamato, *Appl. Opt.* **51**, C1 (2012).
23. Daohong Song, Cibo Lou, Liqin Tang, Zhuoyi Ye, Jingjun Xu, Zhigang Chen, *Int. J. Optics* **27385** (2012).
24. A. Yu. Okulov, *J. Mod. Optics* **2**, 241 (2008).
25. T. Fadeyeva, A. Rubass, I. Valkov, A. Volyar, *J. Opt.* **14**, 044020 (2012).
26. A. P. Prudnikov, Yu. A. Brychkov, O. I. Marichev. *Integrals and Series* (Gordon & Breach Science Publishers/CRC Press, 1992), Vol. 1–5, p. 615.
27. V. V. Kotlyar, A. A. Kovalev, V. A. Soifer, *Comp. Opt.* **38**, 410 (2014)
28. M. V. Berry, M. R. Jeffrey, *Prog. Opt.* **50**, 13 (2007).
29. M. V. Berry, M. R. Jeffrey, J. G. Lunney, *Proc. R. Soc. A* **462**, 1629 (2006).
30. I. Skab, Yu. Vasylkiv, V. Savaryn, R. Vlokh, *J. Opt. Soc. Am. A* **28**, 633 (2011).
31. I. Skab, Yu. Vasylkiv, V. Savaryn, R. Vlokh, *Ukr. J. Phys. Opt.* **11**, 193 (2010).
32. T. A. Fadeyeva, C. N. Alexeyev, P. M. Anischenko, A. V. Volyar, *Appl. Opt.* **51**, C1 (2012).
33. Yu. A. Egorov, T. A. Fadeyeva, A. V. Volyar, *J. Optics A: Pure and Appl. Opt.* **6**, S217 (2004).
34. N. S. Kazak, N. A. Khio, A. A. Ryzhevich, *Quantum Electron.* **29**, 1020 (1999).
35. V. Belyi, T. King, N. Kazak, N. Khio, E. Katranji, A. Ryzhecich, *Proc. SPIE* **4403**, 229 (2001).
36. V. N. Belyi, N. Khilo, *J. Opt.* **15**, 4018 (2013).
37. T. King, W. Hogervorst, N. Kazak, N. Khilo, and A. Ryzhevich, *Opt. Commun.* **187**, 407 (2001).
38. N. A. Khilo, *Opt. Commun.* **286**, 1 (2013).

ДРОБНЫЕ ОПТИЧЕСКИЕ ВИХРИ: УСТОЙЧИВОСТЬ И ПРЕОБРАЗОВАНИЕ

Воляр А. В., Алексеев К. Н., Егоров Ю. А., Акимова Я. Е. *

Физико-технический институт, Крымский федеральный университет имени В. И. Вернадского, Симферополь 295007, Россия
****E-mail:** yana_akimova_1994@mail.ru*

В данной работе мы изучили формирование и эволюцию сингулярных пучков, переносящих оптические вихри с дробным топологическим зарядом как в однородной, так и неоднородной анизотропной среде. Вихри дробного порядка могут быть представлены как суперпозиция бесконечного числа вихрей целочисленного порядка с определенным распределением энергии (вихревые спектры). В работе показано, что гладкий волновой фронт вихря с дробным топологическим зарядом может распадаться на асимметричный массив целых вихрей, либо наоборот, массив оптических вихрей может образовывать гладкий геликоидальный волновой фронт. Показано, что наложением конечного числа вихревых пучков дробного порядка можно сформировать пучки с произвольными значениями топологических зарядов. Мы продемонстрировали, что в двухосных кристаллах при условии конической дифракции дробные вихри не устойчивы, а также, что кольцевые массивы волокон с пространственной вариацией двулучепреломления являются подходящей средой для вихревых пучков дробного порядка.

Ключевые слова: оптически вихри, дробный топологический заряд, супермоды дробного порядка, скрытая фаза, массив оптических вихрей.

Список литературы

1. Soskin M. S., Vasnetsov M. V., Singular optics // Prog. Opt. 2001. Vol. 42. P. 219.
2. Basisty I., Soskin M., Vasnetsov M., Optical wavefront, dislocations and their properties // Opt. Commun. 1995. Vol. 119. P. 604.
3. Synthesis and analysis of optical vortices with fractional topological change / Basisty I., Slyusar V., Soskin M., et al. // J. Opt. A-Pure Appl. Op. 2004. Vol. 6. P. 166.
4. Wavefront dislocations in the Aharnov-Bohn effect and its water wave analogue / Berry M. V., Chambers R. G., Large M. D. et al. // Eur. J. Phys. 1980. Vol. 1. P. 154.
5. Berry M. V., Optical vortices evolving from helicoidal integer and fractional phase steps // J. Optics. A. 2004. Vol. 6. P. 259.
6. Volovik G. E., Mineev V. P., Linear and point peculiarities in superfluid H^3 // Pis'ma Zhurnal. Eksp. Teor. Fiziki. 1976. Vol. 24. P. 605.
7. Observation of Half-Height Magnetization Steps in Sr_2RuO_4 / J. Jang et al. // Science 2011. Vol. 331. P. 186.
8. Periodic shedding of vortex dipoles from a moving penetrable obstacle in a Bose-Einstein condensate / Seo S. W., Kang S., Know W. J., and Yong-il Shin // Physical Review A. 2015. Vol. 92. P. 033613.
9. J. A. Sauls, Viewpoint: Half-Quantum vortices in superfluid helium // Physics. 2016. Vol. 9. P. 148.
10. Hansen A., Schuliz J. T., Bigeliw N. P., Singular atom optics with spinor Bose-Einstein condensates // Optica. 2016. Vol. 3(4), P. 355.
11. Tao S., Lee W., Yuan X., Experimental study of holographic generation of fractional Bessel beams // Appl. Opt. 2004. Vol. 43. P. 122.
12. Leach J., Yao E., Padgett M. J., Observation of the vortex structure of a non-integer vortex beam // New J. Phys. 2004. Vol. 6. P. 71.
13. Garcia H., Diffraction of plane waves by finite radius spiral phase plates of integer and fractional topological cgange // J. Gutierrez-Vega, J. Opt. Soc. Am. A. 2009. Vol. 26. P. 794.
14. Gutiérrez-Vega J. C., López-Mariscal C., Nondiffracting vortex beams with continuous orbital angular momentum order dependence // J. Opt. Soc. Am. A. 2008. Vol. 10. P. 015009.
15. Mitri F. G., Vector wave analysis of an electromagnetic high-order Bessel vortex beam of fractional type // Opt. Lett. 2011. Vol. 36. P. 606.
16. Magnet-controlled surface defect modes of photonic crystal / Yiqi Fang et al. // Phys. Rev. A. 2017. Vol. 95, P. 023821.
17. Vector erf-Gaussian beams: fractional optical vortices and asymmetric TE and TM modes / Fadeyeva T. A., Alexeyev C. N., Rubass A., Volyar A. V. // Opt. Lett. 2012. Vol. 37. P. 1397.
18. Does the optical angular momentum change smoothly in fractional charged vortex beams? / Fadeyeva T. A., Alexeyev C. N., Rubass A., Volyar A. V. // Journal of the Optical Society of America B. 2014. Vol. 31. P. 798.
19. Maleshkov G., Neshev D., Dreischuh A., Nonlinear beam steering by fractional vortex dipoles // Phys. Rev. A. 2009. Vol. 80, P. 053828.

20. Transmission of fractional topological change via circular arrays of anisotropic fibers / Alexeyev C. N., Kovalyava A. F., Rubass A. F., Volyar A. V., Yavorsky M. A. // Opt. Lett. 2017. Vol. 42. P. 783.
21. Kiselev A. P., New structures in paraxial Gaussian beams // Opt. Spectrosc. 2004. Vol. 96. P. 479.
22. Polarization pattern of vector beams generated by q-plates with different topological changes / Cardano F., Karimi E., Slussarenko S., Marrucci L., Corrado de Lisio, Santamato E. // Appl. Opt. 2012. Vol. 51. P. 1.
23. Experiments on linear and nonlinear localization of optical vortices in optically induced photonic lattices / Daohong Song, Cibo Lou, Liqin Tang, Zhuoyi Ye, Jingjun Xu, Zhigang Chen // Int. J. Optics 2012. ID 27385. P. 10.
24. Okulov A. Yu., 3D-vortexlabyrnths in the near field of solid-state microchip laser // J. Mod. Optics 2008. Vol. 52(2). P. 241.
25. Fractional optical vertical in a uniaxial ryatal / T. Fadeyeva, A. Rubass, I. Valkov, A. Volyar // J. Opt. 2012. Vol. 14, 044020.
26. Prudnikov A. P., Brychkov Yu. A., Marichev O. I., Direct laplace transforms // Integrals and Series : Gordon & Breach Science Publishers/CRC Press, 1992. Vol. 1–5. P. 615.
27. Kotlyar V. V., Kovalev A. A., Soifer V. A., Diffraction free asymmetric elegant Bessel beams with fractional orbital angular momentum // Comp. Opt. 2014. Vol. 38. P. 4.
28. Berry M. V., Jeffrey M. R., Conical diffraction: Hamilton's diabolical into at the heart of crystal optics // Prog. Opt. 2007. Vol. 50. P. 13.
29. Berry M. V., Jeffrey M. R., Lunney J. G., Conical diffraction: observations and theory // Proc. R. Soc. A 2006. Vol. 462. P. 1629.
30. Optical anisotropy induced by torsion stresses in $LiNbO_3$ crystals: Appearance of an optical vortex / Skab I., Vasylkiv Yu., Savaryn V., Vlokh R. // J. Opt. Soc. Am. 2011. Vol. 28. P. 633.
31. Skab I., Vasylkiv Yu., Savaryn V., Vlokh R., Relations for optical indicatrix parameters at the crystal torsion // Ukr. J. Phys. Opt. 2010. Vol. 11. P. 193.
32. Engineering of the space-variant linear polarization vortex-beams in biaxially induced crystals / Fadeyeva T. A., Alexeyev C. N., Anischenko P. M., Volyar A. V. // Appl. Opt. 2012. Vol. 51. C1.
33. Egorov Yu. A., Fadeyeva T. A., Volyar A. V., Fine structure of singular beams in crystals: colors and polarization // J. Optics A: Pure and Appl. Opt. 2004. Vol. 6. P. 217.
34. Kazak N. S., Khio N. A., Ryzhevich A. A., Generation of Bessel light beams under the conditions of internal conical refraction // Quantum Electron. 1999. Vol. 29. P. 1020.
35. Methods of formation and nonlinear conversion of Bessel optical vortices / V. Belyi, T. King, N. Kazak, N. Khio, E. Katranji, A. Ryzhecich, // Proc. SPIE 2001. Vol. 4403. P. 229.
36. Belyi V. N., Khilo N., Spin-to-orbital angular momentum conversion for Bessel beams propagating along the optical axes of homogeneous uniaxial and biaxial crystals // J. Opt. 2013. Vol. 15. P. 4018.
37. Formation of higher-order Bessel light beams in biaxial crystals / King T., Hogervorst W., Kazak N., Khilo N., Ryzhevich A. // Opt. Commun. 2001. Vol. 187. P. 407.
38. Khilo N. A., Conical diffraction and transformation of Bessel beams in biaxial cryctals // Opt. Commun. 2013. Vol. 286. P. 1.

Поступила в редакцию 22.06.2017 г. Принята к публикации 26.11.2017 г.
Received June 22, 2017. Accepted for publication November 26, 2017